JOURNAL OF
EMERGING INVESTIGATORS

Article

Effects of microconvection on bubble displacement during water electrolysis under microgravity

Alex Gu[1], Canis Li[1], Jamin Xie[1], Daisy Zeng[1], Kingshuk Daschowdhury[1], Leon Yee[1], Yitian Li[1], Austin Chiang[1], Emeka Okekeocha[1]

[1] Valley Christian High School, San Jose, California

SUMMARY

Water electrolysis is the electrochemical process of passing an electrical current through water to separate it into hydrogen and oxygen gases at two electrodes. The hydrogen and oxygen gas bubbles produced during water electrolysis are displaced from the electrodes by two classes of phenomena, which we categorize as either buoyancy or microconvection. Buoyancy is the phenomenon caused by the upward force exerted by a fluid. We define microconvection as the effects of non-buoyant bubble-displacing phenomena, such as Brownian motion. We determined the role of microconvection during water electrolysis by comparing the formation and behavior of gas bubbles under both terrestrial gravity (1G) on Earth and microgravity (μG) aboard the International Space Station. During water electrolysis under 1G, buoyancy-induced macroconvection dominates microconvection attributed to non-buoyant forces. The accumulation of gas bubbles can impede the contact of the buffer solution and platinum electrode, hindering the current flow for further electrolysis. We studied this phenomenon with a camera and current sensor. We hypothesized that microconvection has a weaker effect in displacing bubbles compared to buoyancy and that the current will decrease more over time under μG due to extended contact of the gas bubbles with the electrodes during electrolysis. Our results showed that microconvection plays a non-negligible role in bubble displacement in water electrolysis, a finding which has broad applications, including zero-pollution hydrogen production and hydrogen fuel cells.

INTRODUCTION

Water electrolysis is defined as the electrochemical process of passing an electrical current through water to separate it into hydrogen and oxygen gases. Electrolysis can be broken into two half-reactions occurring either at the negatively charged cathode or the positively charged anode. When a sufficient voltage is applied across the electrodes, reduction occurs at the cathode, producing hydrogen gas bubbles, and oxidation occurs at the anode, producing oxygen gas bubbles. This can be summarized as follows:

Oxidation (anode): $2H_2O(l) \rightarrow O_2(g) + 4H^+(aq) + 4e^-, E^o_{ox} = -1.23\,V, E^o_{red} = 1.23\,V$

Reduction (cathode): $2H^+(aq) + 2e^- \rightarrow H_2(g), E^o_{red} = 0.00\,V$

Overall reaction: $2H_2O(l) \rightarrow O_2(g) + 2H_2(g), E^o_{cell} = -1.23\,V$

Where E^o_{ox} = standard oxidation potential (under standard conditions), E^o_{red} = standard reduction potential (under standard conditions), and E^o_{cell} = standard cell potential (potential difference between the cells), the difference of the reduction potentials of the two half-reactions. Note that removing the "°" symbol in each potential represents non-standard conditions.

Faraday's law of electrolysis states that the rate of electrolysis is directly related to the current between the electrodes since the amount of gases formed is proportional to the total charge passed. The reaction requires 1.23*V* applied, but high overpotentials caused by the evolving gas substantially increase the actual voltage needed (1, 2).

Water electrolysis can be modeled using the Nernst equation, $E = E^o - \frac{RTln(Q)}{nF}$, where *E* represents either the reduction or oxidation potential of a half-reaction, *R* is the universal gas constant, *T* is the temperature, *Q* is the reaction quotient describing reaction progress, *n* is the moles of electrons transferred per moles of reaction, and *F* is the Faraday constant. Note that the if E_{red} is used in the Nernst equation, then *Q* must be calculated with the reaction written as a reduction reaction, and vice versa for oxidation. As the reaction progresses, reactants are consumed, products are formed, and pH is shifted, leading to an increase of *Q*. This corresponds to a decrease in because E^o, the standard potential, is constant. Therefore, higher voltage is required for the reaction to proceed, so current is expected to decrease over time by Ohm's law.

To elaborate, the H^+ ion is the only aqueous species in both the oxidation and reduction reactions, so $Q = [H^+]^4$ and $[H^+]^{-2}$ for the oxidation and reduction reactions, respectively. Therefore, $\frac{\ln(Q)}{n} = \ln([H^+])$ for oxidation and $\frac{\ln(Q)}{n} = -\ln([H^+])$ for reduction, as n = 4 for oxidation and n= 2 for reduction. Considering the two reactions separately, by the Nernst equation, E_{ox} becomes more negative for the oxidation reaction and E_{red} becomes more negative for the reduction reaction because H^+ increases at the anode (oxidation) and decreases at the cathode (reduction). Thus, E_{cell} becomes more negative over time.

Traditionally, water electrolysis is conducted using a porous membrane, allowing ions to pass through without bulk-mixing of the solutions. Mixing can produce an undesirable reaction between hydrogen and oxygen gas. A salt bridge can be used in place of a porous membrane by gellifying a conductive salt solution through a gelling agent such as agar-agar. If the chambers are separated with a salt bridge, ion flow should be slow enough to allow the two sides to maintain a distinct pH. Thus, the pH of the electrolyte solution will decrease at the anode and increase at the cathode, caused by the production or consumption of hydrogen ions.

The oxygen and hydrogen gas bubbles produced during water electrolysis do not perpetually remain on the electrodes. This is due to the presence of bubble-displacing phenomena, which we categorize as either buoyancy or microconvection.

Buoyancy is the phenomenon caused by the upward force exerted by a fluid. We define microconvection as the effects of non-buoyant bubble-displacing phenomena, such as Brownian motion, which is the random thermal motion of particles in a medium such as a fluid. Under terrestrial gravity (1G) on Earth, gas bubbles formed on the surface of the electrodes are typically displaced by buoyancy-induced macroconvection, dominating the effects of microconvection (1). Under microgravity (μG), referring to an environment with very weak effective gravity, the presence of a significant buoyant force is lost, and thus the motion of the bubbles is primarily affected by microconvection. As more oxygen and hydrogen is produced, the gas bubbles build up on the surface of the electrode, decreasing the area of the interface between the electrode and solution. Because the rate of electrolysis is directly related to the available electrode surface area, the current falls over time.

The International Space Station (ISS) uses water electrolysis to generate its own oxygen, so an understanding of water electrolysis in a μG environment is necessary to produce oxygen efficiently on the ISS. Oxygen production is important in many life support systems (LSS), including systems that are plant-based and systems for deep-space habilitation capabilities. ISS LSS systems supply, recover, and recycle oxygen to prevent hazardous chemicals such as ammonia and acetone, products of both human emission and chemical experiments, from accumulating (3). A better understanding of the role that microconvection of accumulated oxygen and hydrogen gases plays in water electrolysis will allow us to develop more efficient and effective water electrolysis plants. Water electrolysis also contributes to zero-pollution hydrogen production, the process which leads to storing chemical energy in the form of fuel cells. The long-term effects of storing hydrogen (H_2) as fuel lead to decreased greenhouse gas emissions and excess stored energy in comparison to alternative renewable sources such as solar energy, wind energy, etc (4). Applications of hydrogen gas include cooling electric generators and reducing atmospheres for heat-treatment processes (5).

In this study, because buoyancy depends on the effective gravity and is thus negligible under μG but significant under 1G, we hypothesized that microconvection is the dominant force in displacing bubbles under μG while buoyancy is the dominant force under 1G. Additionally, microconvection under μG is a significant but weaker phenomenon compared to buoyancy under 1G. Thus, under μG, the gas bubbles will remain on the platinum electrodes for a longer period of time compared to under 1G, thereby reducing contact of the electrode with the electrolyte, hindering gas production, and leading to a greater drop in current over time. Also, as electrolysis progresses, the cell potential required further increases as H^+ ions are depleted from the cathode and accumulated in the anode. By the Nernst equation, the cell potential decreases, increasing in magnitude. This has the effect of decreasing the current when fixed voltage is applied. This would decrease the overall rate of electrolysis throughout subsequent trials. To test our hypotheses, we conducted experimental trials using custom-built electrolysis chambers: one under 1G on Earth and one under μG aboard the ISS. Our findings suggest that microconvection plays a non-negligible but weak role in gas displacement under μG. Furthermore, efficiency in water electrolysis systems under μG environments could be improved by mechanically promoting gas displacement.

RESULTS

In this study, we compared the effects of microconvection and buoyancy during water electrolysis under 1G and μG. We quantitatively analyzed the electrode current measured over time from a current sensor, and qualitatively analyzed camera photos of our custom-built electrolysis chamber. Although we could not directly measure the effects of microconvection and buoyancy in bubble displacement, the electrode current is a good indicator of this as suggested by Faraday's law.

We obtained the time series of current measurements of the electrolysis trials conducted in phosphate buffer solution under 1G and μG. We then performed least squares regression on them with an exponential model (**Figure 1**), as predicted from our proposed differential equation model described in the **Discussion**. Although all the trials exhibited strong exponential model fits, we chose to restrict our analysis to trials where the measurement interval was eight seconds, as this allowed us to analyze whether the exponential model persisted over longer timespans. Under both 1G and μG, the currents decreased exponentially, reaching an asymptote after a characteristic time scale, on electrode saturation. The asymptote represents a steady state current, where the rate of microconvection or buoyancy-induced bubble displacement matches the rate of bubble formation from electrolysis. The steady state current was on average 1.5 mA below the initial current value under μG and 0.5 mA below the corresponding value under 1G, demonstrating a wider range of current values over the course of the experiment under μG than 1G. Additionally, the initial current values under μG were lower than under 1G by around 1 mA (**Table 1**).

To qualitatively observe the behavior of the gas, photos of the chamber were taken before and after electrolysis trials in one hour intervals under μG (**Figure 2**). Hydrogen gas was formed on the cathode in the right half of the chamber, and oxygen gas was formed on the anode in the left half. As expected by stoichiometry, approximately twice as much hydrogen gas was produced compared to oxygen. Unlike the hydrogen bubbles, the oxygen bubbles tended to form clumps, leaving gaps on the electrode surface. Under μG, most of the

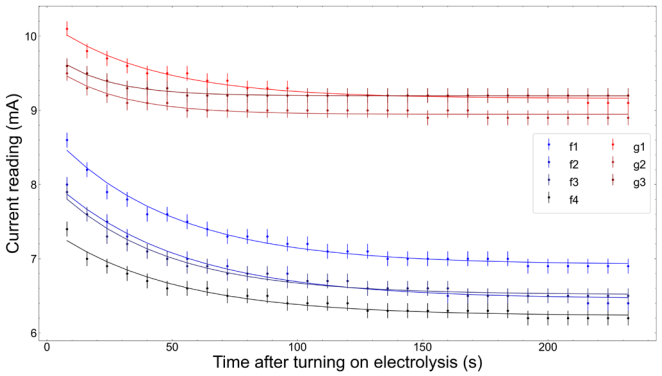

Figure 1: Current during electrolysis under μG (blue) and 1G (red). For each trial, an exponential fit, $I(t)=Ae^{-Bt}+C$, is plotted as well. Trials indexed with f and g represent μG and 1G, respectively. Only data where the measurement period was eight seconds was plotted. Trials under μG and 1G were conducted independently every 5 days and 5 hours respectively. Trials were numbered according to the date conducted. The exponential least-squares fit model was plotted for each trial. The error bars refer to the uncertainty of sensor measurement (0.1 mA)

Trial	A	B	C	A_err	B_err	C_err	R^2
f1	1.8206	0.0210	6.9208	0.0982	0.0023	0.0375	0.9828
f2	1.6521	0.0196	6.4579	0.0938	0.0024	0.0401	0.9776
f3	1.5471	0.0230	6.5159	0.1047	0.00294	0.0344	0.981
f4	1.1950	0.0206	6.2309	0.0972	0.0034	0.0381	0.9627
g1	1.0353	0.0241	9.1600	0.1084	0.0046	0.03301	0.9673
g2	0.6983	0.0384	8.9468	0.1567	0.0122	0.0251	0.9004
g3	0.6140	0.0484	9.1966	0.1944	0.0198	0.0232	0.9777

Table 1: Exponential least-squares fit parameters for current *I(t)* as a function of time: $I(t)=Ae^{-Bt}+C$. Parameter values for **A, B, C,** and the corresponding standard errors, along with R-squared values. Trials indexed with f and g represent μG and 1G, respectively. Trials were numbered in the same order as the date were conducted. The terrestrial trials were all conducted on the same day because bubbles displaced immediately and there was no need to reset the chamber with the vibrator motor. Overall, both the initial and steady state currents decreased gradually over the course of the experiment, supporting our secondary hypothesis that as electrolysis progressed, the cell potential required would further increase in magnitude as H^+ ions are depleted from the cathode and accumulated in the anode.

bubble froth layer dispersed over the first hour after electrolysis was turned off due to the vibrator motor, with few residual bubbles remaining after 24 hours. Between trials, the color of the pH indicator did not change discernibly.

The shift in the exponential fit of the current across the duration of each trial was also measured (**Table 1**). Overall, both the initial and steady state currents decreased gradually over the course of the experiment. The initial current decreased from 8.6 to 7.4 mA under μG, and from 10.1 to 9.6 mA under 1G. The steady state current under μG decreased from 6.92 to 6.23 mA, as predicted by the Nernst equation, since the cell potential decreases with the shift in pH. However, the steady state current under 1G fluctuated around 9 mA under 1G.

DISCUSSION

We hypothesized that the effects of microconvection under μG are weaker but not negligible compared to buoyancy under 1G during water electrolysis. We ran autonomous water electrolysis experiments both on Earth under 1G and aboard the ISS under μG. Our experiment collected quantitative data in the form of current measurements and qualitative data in the form of camera photos. Our findings support our hypothesis and can be used design more effective water electrolysis systems under both 1G and μG but especially under the latter where microconvection is dominant.

We found that the current decreased exponentially with time, approaching an asymptotic value. Under 1G, this asymptotic behavior can be explained by the rate of bubble production eventually matching the rate that bubbles rise off the electrode due to the buoyant force. Under μG, this can be attributed to microconvection displacing the bubbles, replenishing the contact between the electrode and electrolyte. The wider difference between the initial and asymptote current for μG suggests that the rate of microconvection is slower than rate of buoyancy-driven convection.

Following the exponential model predicting the asymptotic behavior of the current established in **Materials and Methods**, almost all obtained fits had coefficients of determination (R^2) values over 0.95, indicating a strong correlation and supporting the plausibility of this model (**Table 1**). The change in the model parameters were recorded throughout the course of the experiment, with a gradual, but significant decrease in both the initial current ($A + C$) and the steady-state current (C), while the time scale (B) remained relatively constant (**Table 1**). For example, the steady-state current (C), dropped from 6.92 mA at the first trial to just 6.23 mA at the final trial under μG, with a similar effect for the coefficient A. This supports our hypothesis that the shift in H^+ concentration causes the cell potential to decrease and its magnitude to increase by the Nernst equation, which has the effect of decreasing the current when fixed voltage is applied. The values of $A + C$ were greater overall for the ground trials as the experiment progressed, which suggests that, looking at the beginning of each flight trial except the first, residual bubbles from the previous flight trial caused additional impedance. However, our results show that the time scale of microconvection is not affected by the initial current at the start of each trial.

Furthermore, C was never zero over all our trials, which demonstrates the influence of microconvection: If there was no net displacing force, the steady-state current would be

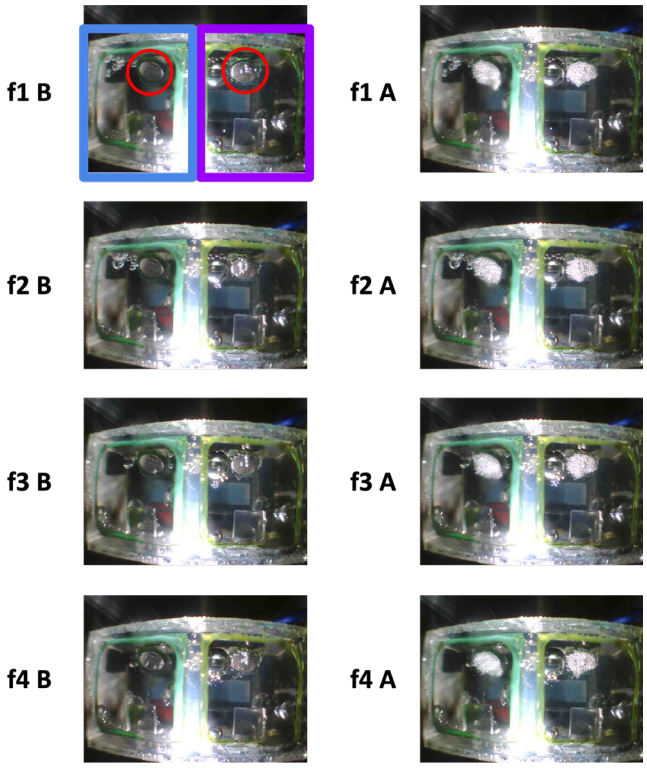

Figure 2. Pictures before and after electrolysis trials under μG. Trials are indexed with f, representing μG. Trials were numbered according to the date conducted. The panel letter "B" represents before electrolysis, and "A" represents immediately after. The anode is in the left half of the chamber, and the cathode is in the right. The green and yellow buildup are the pH indicator, bromothymol blue. Bubble formation can be seen immediately after electrolysis (f1 A through f4 A). Pictures under 1G were not taken because buoyancy displaced the bubbles almost immediately. In f1 A, note that the blue box indicates the anode, the purple box indicates the cathode, and the red circles contain the bubble formation sites.

zero after solving the differential equation stated above. In other words, the parameter *q*, which characterizes bubble displacement due to convection, being zero in the differential equation implies that *C* is zero, and vice versa.

Additionally, the relative difference (*A*) between the steady state current (*C*) and the initial current (*A* + *C*) was greater under μG than microconvection and convection. This is because as expected, the effects of microconvection under μG were weaker at displacing bubbles than buoyancy under 1G. We show this quantitatively: the fit parameter *A* can be expressed as $kA_0\left(\frac{p}{p+q}\right)$. As *k* and *p* are constants attributed to the electrolysis reaction, they are expected to be the same whether performed under μG or 1G. Plotting the function $\frac{p}{p+q}$ as a function of *q* with *p* held constant yields that A is monotonically decreasing as *q* increases, *i.e.*, weaker convection leads to a wider gap.

Overall, our quantitative data were limited by the 0.1mA precision of our current sensor, which led to possible variations in the accuracy of the exponential fit. A more precise treatment of the various bubble-displacing phenomena such as surface tension and Brownian motion could provide more physical insights to our model. Each experimental trial was approximately three hours longer than a day, resulting in the trials not being perfectly 5 days spaced as expected by our measurement period cycling. However, the time between trials has no effect on the quantitative and qualitatitive results observed.

Now we discuss our qualitative data. Our camera took pictures before and after electrolysis trials under μG, with 24 hours in between each trial (**Figure 2**). Pictures under 1G were neglected because buoyancy displaced the bubbles almost immediately. We observed that the bubble froth layer almost completely dispersed on both electrodes between trials despite there being approximately twice as much hydrogen gas produced as oxygen gas. However, more hydrogen gas bubbles remained compared to oxygen, which can be attributed to surface tension between the bubble and electrode dominating for smaller length scales (6).

Our qualitative observations were limited by the camera not focusing on the bubbles. Also, changes in pH were not clearly observable through the camera images due to a low concentration of the indicator bromothymol blue and adsorption to the epoxied walls. Further testing of the concentration of bromothymol blue may be explored to find a concentration that is not too high to avoid obscuring camera images, and not too low prevent adsorption of the bromothymol blue to the walls.

Although buoyancy is more influential than microconvection in maintaining the electrode electrolyte contact during electrolysis, our results suggest that microconvection plays a significant role in displacing the bubbles from the electrodes and quantifies the extent of this effect under μG. Having vibrator motors during water electrolysis under μG to further displace bubbles from the electrodes could increase the efficiency of electrolysis and improve existing standard water electrolysis processes.

Future research may involve quantifying the effect of pH on the cell potential and the current, and the effect of different applied voltages on the electrolysis current. Additionally, future experiments could collect additional data to better assess the steady state current under 1G. Further analysis will provide deeper insight into the effects of the water overpotential as well as improving efficiency with respect to voltage.

MATERIALS AND METHODS

Our experiment on water electrolysis was contained in a computer-aided designed (CAD) chamber, separated into two smaller chambers. Each mini-chamber measured 16 x 16 x 18 mm and was completely filled with solution. The chemicals used in the solution – potassium phosphate monobasic and potassium phosphate dibasic – were both of reagent-grade quality. The solution also had a 0.04% w/v solution of bromothymol blue pH indicator, containing a 95% dye concentration. The entire chamber was epoxy-coated on both the inside and outside to prevent water leakage. Each electrode measured 5 mm in diameter and 0.1 mm thick, and sat on a 2 mm platform tilted 45°, attached to the center of its respective chamber wall (**Figure 3**). The electrode platforms were designed to showcase the maximum surface area of the electrode to the camera for optimal image analysis. Our μG and terrestrial experiments differed only in the product used to print the chambers (acrylonitrile butadiene styrene and resin filament, respectively) and the placement of the LEDs for camera lighting; these variable changes are not expected to affect the results of the experiment.

Initially, two chambers were filled with an electrolyte solution, one consisting of 0.02 M potassium phosphate dibasic and the other 0.02 M potassium phosphate monobasic (Sigma Aldrich), thus acting as a buffer when electrolysis occurs. A neutral electrolyte, 0.7 M potassium sulfate (Fisher Scientific), was added to increase electrical conductivity. 0.04 w/v% of bromothymol blue (Sigma Aldrich) was dissolved in the water as a pH indicator. These two chambers were electrically connected via a 0.7 M potassium sulfate salt bridge gellified with 2 w/v% agar (Agarose from Benchmark Scientific) (**Figure 3**). The salt bridge allows current to pass between the electrodes while keeping the solutions separate and to keep the evolved hydrogen and oxygen gases apart. Platinum was used as an inert electrode for both the cathode and anode as it does not react with other ions in the solution (Refining Systems, Inc.). Gas evolved was displaced into a connected fluid bag to prevent pressure buildup.

Throughout the course of 30 days, 30 trials of various durations were conducted autonomously aboard the ISS under μG and on Earth under 1G, with the experiment initiation

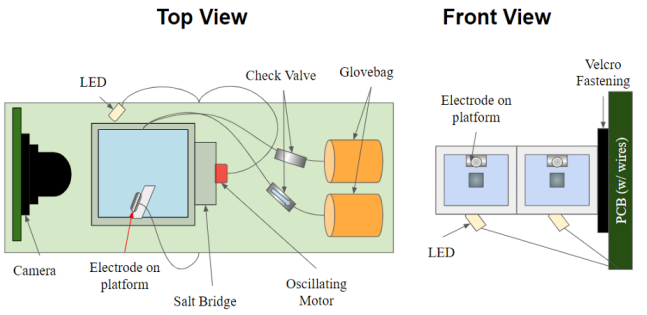

Figure 3: Experiment block diagram. Pictured is the block diagram of the experiment, detailing the relative positions of the components used. The Top View displays the components from the top, while the Front View displays from the camera's point of view.

and data collection controlled by PBasic software. The magnitude and direction of the local gravitational acceleration of the chamber was not measured while on the ISS since we assumed the effects of μG (on the order of 10 micro Gs) to be negligible compared to microconvection. Each day, a fixed voltage of 5 V was applied across the electrodes and the current was measured 30 times at a constant period. The sensor produced measurements with a resolution of 0.1 mA; thus, for each measurement, an uncertainty of 0.1 mA was used. The measurement period was varied on each day according to a five day cycle: 0.5, 1, 1.5, 3, and 8 seconds between measurements. Pictures of the electrode surface were taken immediately before and after electrolysis occurred, allowing the behavior of the gas to be qualitatively observed (https://github.com/VCHS-IRL-Team-H-21-22/water-electrolysis).

We propose an exponential decay model for the measured electrolysis current over time. By Faraday's Law, the current is directly proportional to the effective surface area: $I(t) = kS(t)$, defined as the area of the electrode not covered by bubbles, i.e., the area available for reactions. Its rate of change, $\frac{dS}{dt}$, can be attributed to a combination of gas formation from electrolysis and bubble displacement from buoyancy/microconvection. We consider these two effects separately first. According to collision theory, in general rate of reaction increases with increasing surface area (7). Thus we propose that the rate of reaction and thus rate of gas formation is proportional to the area available to react, i.e. $\frac{dS}{dt} = -ps$ for some constant p. We propose the rate of bubble displacement from convection is similarly proportional to the area covered by bubbles, $\frac{dS}{dt} = q(S_0 - S)$ i.e. where q is a constant and S_0 is the total area of the electrode. Combining these two effects, we have $\frac{dS}{dt} = -ps + q(S_0 - S) = -(p+q)S + qS_0$. Defining $r = p + q$ as the time scale of the electrolysis, we have $\frac{dS}{dt} = -rS + qS_0$. The solution to this differential equation is exponential: $S(t) = S_0\left(\frac{q}{r} + \left(1 - \frac{q}{r}\right)e^{-rt}\right)$, and plugged into Faraday's Law gives the current in the form $I(t)=Ae^{-Bt}+C$.

ACKNOWLEDGEMENTS

We would like to thank our mentors Marcell Marc, Howell Ivy, Dan Saldana, George Sousa, and Sandeep Shah for their valuable support throughout our experiment. Additionally, we thank David Kyser for assisting us in the manuscript revision process. Our deepest gratitude also goes out to Refining Systems, Inc., who donated the platinum electrodes used in our experiment—without their help, we would not have been able to complete our experiment.

Received: October 11, 2022
Accepted: April 10, 2023
Published: August 20, 2023

REFERENCES

1. Matsushima, Hisayoshi, et al. "Water electrolysis under microgravity: Part 1. Experimental technique." *Electrochimica Acta*, vol. 48, no. 28, 15 Dec. 2003, https://doi.org/10.1016/s0013-4686(03)00579-6.
2. Matsushima, Hisayoshi, et al. "Water electrolysis under microgravity: Part II. Description of gas bubble evolution phenomena." *Electrochimica Acta*, vol. 51, no. 20, 25 May 2006, https://doi.org/10.1016/j.electacta.2005.11.046.
3. "Breathing Easy on the Space Station." *NASA*, NASA, 12 Nov. 2000.
4. Wang, Shan, et al. "Hydrogen production from water electrolysis: role of catalysts." *Nano Convergence*, vol. 8, no. 4, 11 Feb. 2021, https://doi.org/10.1186/s40580-021-00254-x.
5. K. Scott. "Membranes for Electrochemical Cells." Handbook of Industrial Membranes, 2 Sept. 2007, pp 773-790.
6. Lautrup, B. "Physics of Continuous Matter: Exotic and Everyday Phenomena in the Macroscopic World." 2nd ed., CRC Press, 2019, Ch. 5.
7. Alviar-Agnew, Marisa, and Henry Agnew. "15.2: The Rate of a Chemical Reaction." Chemistry LibreTexts, 16 Sept. 2022.
8. Kaneko, Hiroko, et al. "Water electrolysis under microgravity condition by parabolic flight." *Electrochimica Acta*, vol. 38, no. 5, April 1993, https://doi.org/10.1016/0013-4686(93)80245-U.
9. Odufalu, Florence-Damilola, et al. "2.5: Reaction Rate." *LibreTexts*, chem.libretexts.org/Bookshelves/Physical_and_Theoretical_Chemistry_Textbook_Maps/Supplemental_Modules_(Physical_and_Theoretical_Chemistry)/Kinetics/02%3A_Reaction_Rates/2.05%3A_Reaction_Rate
10. Wenzel, Thomas. "5. Electrochemical Cells." *LibreTexts*, chem.libretexts.org/Bookshelves/Analytical_Chemistry/Supplemental_Modules_(Analytical_Chemistry)/Analytical_Sciences_Digital_Library/In_Class_Activities/Electrochemical_Methods_of_Analysis/02_Text/5._Electrochemical_Cells
11. Doan, Tuan Linh, et al. "A review of the porous transport layer in polymer electrolyte membrane water electrolysis." International Journal of Energy Research, vol. 45, no. 10, 17 April 2021, https://doi.org/10.1002/er.6739.

APPENDIX

Event Table PBASIC code (https://github.com/VCHS-IRL-Team-H-21-22/water-electrolysis): Each row in the table is a time-stamp for the software to perform various events such as taking photos and running current. The final row resets the time back to before row 2, allowing the table to be run multiple times automatically.

Day	Hour	Min	Tag	Eventbyte	Comment
00	00	00	$FF	00	'Row 0 Do Nothing
00	13	00	$FF	05	'Row 1 Set config
01	00	00	$FF	01	'Row 2 Take photo
01	00	15	$FF	02	'Row 3 Turn on and Measure current for x seconds (take photo)
01	00	25	$FF	03	'Row 4 Turn on vibrator motor
01	01	00	$FF	01	'Row 5 Take photo
01	02	00	$FF	01	'Row 6 Take photo
01	03	00	$FF	01	'Row 7 Take photo
01	04	00	$FF	01	'Row 8 Take photo
01	05	00	$FF	01	'Row 9 Take photo
01	06	00	$FF	01	'Row 10 Take photo
01	07	00	$FF	01	'Row 11 Take photo
01	08	00	$FF	01	'Row 12 Take photo
01	09	00	$FF	01	'Row 13 Take photo
01	10	00	$FF	01	'Row 14 Take photo
01	11	00	$FF	01	'Row 15 Take photo
01	12	00	$FF	01	'Row 16 Take photo
01	13	00	$FF	01	'Row 17 Take photo
01	14	00	$FF	01	'Row 18 Take photo
01	15	00	$FF	01	'Row 19 Take photo
01	16	00	$FF	01	'Row 20 Take photo
01	17	00	$FF	01	'Row 21 Take photo
01	18	00	$FF	01	'Row 22 Take photo
01	19	00	$FF	01	'Row 23 Take photo
01	20	00	$FF	01	'Row 24 Take photo
01	21	00	$FF	01	'Row 25 Take photo
01	22	00	$FF	01	'Row 26 Take photo
01	23	00	$FF	01	'Row 27 Take photo
01	23	59	$FF	04	Row 28 Reset the time to 0D 23H 59M